BasePrompt: Self-Prompting Genome Language Models for RNA Fitness Prediction

Jin Gao[1*], **Zirui Zeng**[1*], **Zheling Tan**[1], **Junhao Shi**[1], **Dequan Wang**[1,2†]
[1]Shanghai Jiao Tong University [2]Shanghai Innovation Institute

Abstract

Genome Language Models (GLMs) pre-trained on trillions of nucleotides already exhibit strong zero-shot RNA fitness predictors, yet they cannot be steered toward a specific assay the way a language model is steered by a prompt. We close this gap by letting GLMs prompt themselves. Our method, BasePrompt, asks GLMs to propose short nucleic-acid prefixes and postfixes that maximally activate the fitness signal for a given sequence. To overcome the causal, forward-only nature of most GLMs, we exploit reverse-complement symmetry and generate upstream as well as downstream prompts without ever updating weights or using labeled variants. For zero-shot RNA fitness prediction on RNAGym, BasePrompt achieves a 6.0% relative improvement over the SOTA Evo2 7B model and 6.6%–16.4% over other GLMs, as measured by Spearman correlation. Auxiliary DNA tasks show the same prompting method compresses native-context information into shorter, model-aligned tokens, boosting pathogenicity classification and next-k-base prediction.

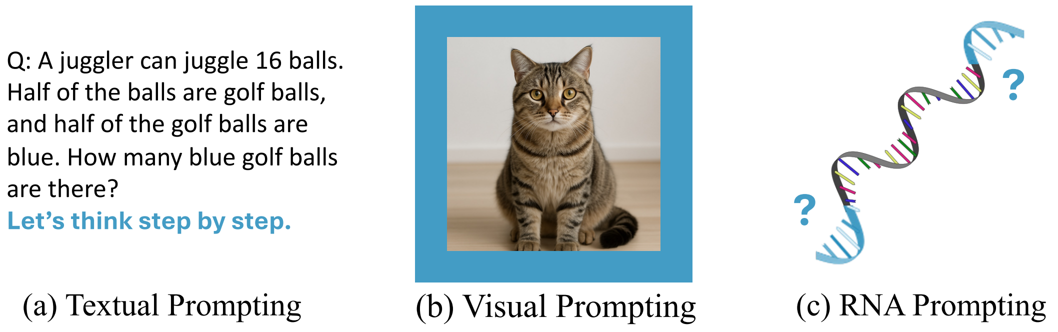
Q: A juggler can juggle 16 balls. Half of the balls are golf balls, and half of the golf balls are blue. How many blue golf balls are there?
Let's think step by step.

Figure 1: Prompting enhances downstream model performance by guiding within the input space, such as (a) textual prompting [25] and (b) visual prompting [5]. However, it is challenging to (c) construct effective prompts for the RNA language.

1 Introduction

Despite impressive zero-shot accuracies on dozens of benchmarks [11, 49, 4], Genome Language Models (GLMs) still lack a steering mechanism comparable to NLP prompt engineering. In transformers for language or vision a short textual phrase ("Let's think step by step") or a handful of learnt continuous tokens is enough to specialise a model without fine-tuning [25, 13, 5, 21], as shown in Figure 1. Genome, however, offers no obvious equivalent: human-readable motifs are not necessarily the primitives that GLMs attend to, and domain-specific fine-tuning violates the zero-shot desideratum of RNA-related competitions [4]. We close this gap by enabling GLMs to write their

[*] Equal contribution. [†] Corresponding author: dequanwang@sjtu.edu.cn.

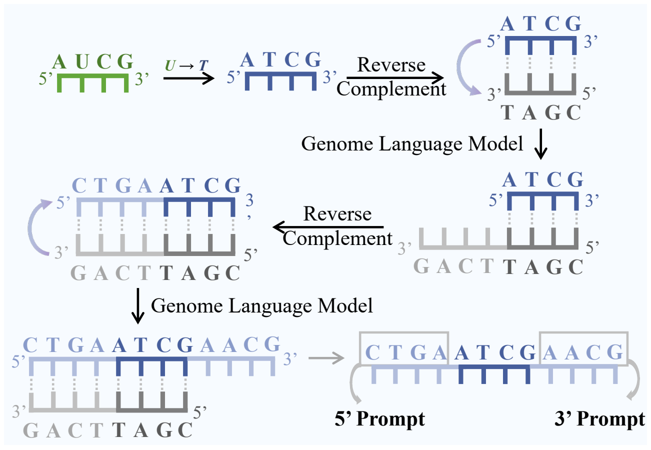

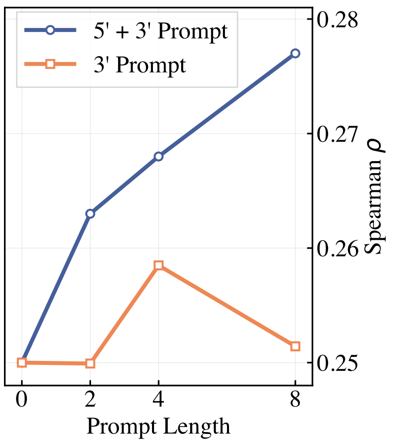

Figure 2: Illustration of BasePrompt. *Left:* It leverages the complementary double-helix structure of DNA to generate upstream ($5'$) and downstream ($3'$) prompts. *Right:* Such a bidirectional prompting has better performance than the pure GLM's downstream prompting in RNA fitness prediction.

own prompts. Concretely, we ask them to propose short nucleic-acid prefixes. By "speaking" to themselves in the native genomic language, GLMs expose statistical regularities opaque to humans yet highly predictive, unlocking specialist behavior in a purely zero-shot regime.

In this paper, we propose a novel mechanism, BasePrompt, for generating both upstream and downstream prompts for a given RNA sequence. As illustrated in the left part of Figure 2, our approach first converts the RNA sequence to its corresponding DNA sequence. To address the unidirectional nature of causal GLMs, which condition only on upstream context, we use the reverse complement principle of DNA for bidirectional prompting, shown to be more effective in inspiring GLMs in RNA fitness prediction [4], as shown in the right panel of Figure 2.

To demonstrate the effectiveness of BasePrompt, we conduct experiments on the RNA fitness prediction benchmark from RNAGym [4], which comprises 70 deep mutational scanning assays and over one million RNA sequences. Our method achieves a relative improvement of 6.0 in Spearman's rank correlation compared with previous state-of-the-art results. Furthermore, BasePrompt is highly efficient, as the short prompting is performed only on the 70 reference RNA sequences, not on each of the one million variants. Our method shows consistent gains across multiple GLMs, including Evo2 7B base, Evo2 7B, and Evo2 40B, suggesting robustness to different models.

We conduct additional DNA experiments primarily for analytical purposes. In a zero-shot classification task using the ClinVar dataset [26], our generated short prompts outperform native genomic prompts, particularly under prompt length constraints. It suggests that while native genomic context may contain redundant information, BasePrompt can generate more condensed and model-aligned prompts for predictive utility. For the next k-base prediction task [49], our upstream prompts guide the model to generate base distributions closer to the native genome.

In summary, our contributions are:

- We introduce BasePrompt, a novel and efficient framework for RNA prompting that leverages GLMs to generate contextual prompts tailored to RNA sequences, significantly improving downstream task performance without requiring additional model training or labeled data.
- Our method establishes a new state-of-the-art in RNA fitness prediction, achieving robust zero-shot improvements on the comprehensive RNAGym benchmark, with consistent performance gains across multiple GLMs in a computationally efficient manner.
- Through auxiliary DNA benchmarks, we demonstrate that prompts generated by BasePrompt are not only highly informationally efficient, but also consistently effective in generative tasks, highlighting their versatility and robustness in biological applications.

2 Related Work

2.1 DNA Reverse Complement in Machine Learning

DNA's inherent double-helical structure [48] implies that both strands carry equivalent genetic information [41, 32, 52]. However, standard machine learning architectures do not inherently account for the reverse complement (RC) symmetry [53, 24, 39, 28, 16]. Existing works employed data augmentation [14] or embed RC symmetry directly into the model architecture [42, 6, 12, 30], though such approaches can face optimization difficulties [51]. In contrast, our BasePrompt method utilizes the reverse complement principle and GLMs for both the upstream and downstream prompt generation for RNA.

2.2 Data Augmentation for DNA

Data augmentation has proven to be a powerful technique in computer vision (CV) and natural language processing to improve model generalization [2, 46]. Augmentations like flipping in CV [50] and synonym substitution in NLP introduce diversity owing to invariance [7]. In genomic modeling, augmentation strategies have been tailored to model training, such as reverse complementation [14], genomic shifting [18, 44], random point mutation [27], and phylogenetic augmentation [19]. In contrast, our BasePrompt adopts the reverse complement and GLMs at test time, requiring no downstream labels, external data, or model tuning.

2.3 In-context Learning in Biology

In-context learning (ICL) is a prominent capability of large language models [31, 1]. Recently, the ICL paradigm has begun to gain attention in bioinformatics applications [33, 29, 20]. Zero-shot prediction has shown particular promise for predicting the functional impact of genetic variants [11, 8, 33]. Some works use crafted natural language instructions and input-output example pairs to steer the model's behavior [22, 47]. Other works tune the model with motif-oriented pretraining [3] or soft prompting [35]. However, existing ICL methods seem not to work universally with model frozen [23, 10]. In contrast, our BasePrompt leverages the pre-trained GLMs for RNA prompting, bypassing the need for natural language instruction or task examples.

3 Method

In this section, we describe our RNA prompting method, BasePrompt, which builds upon the causal framework of a genome language model (GLM), as illustrated in Figure 2. In Section 3.1, we discuss the first tackling when given an RNA sequence and the motivation behind it. In Section 3.2, we introduce the causal modeling of DNA generation by GLMs. In Section 3.3, we introduce how our BasePrompt overcomes the inherent direction limitation.

3.1 Converting RNA to DNA

To construct a meaningful prompt for a given RNA sequence, we first map it back to the genome, where contextual information can be naturally derived by Genome Language Models (GLMs). This step is analogous to inverse transcription [43], enabling the RNA to be localized within its genomic coordinates. Since RNA can be directly processed by DNA-based GLMs after a simple substitution of uracil (U) with thymine (T), we hereafter use DNA as the canonical representation for generality. Building on this formulation, we then analyze an autoregressive model's intrinsic reliance on upstream input and explain how BasePrompt generates bidirectional prompts.

3.2 Autoregressive Model for Genome Sequences

Autoregressive sequence modeling operates on the principle of predicting the next element conditioned on its preceding context. When applied to genome generation, this involves modeling a nucleotide sequence, denoted as $x_1, x_2, \ldots, x_t$, where each token x_i represents a single nucleotide base (*e.g.*, A, T, C, G) or k-mer (*e.g.*, ATGTGG for 6-mer). This modeling is conventionally performed along the $5'$ to $3'$ direction, a choice grounded in fundamental biological processes. The $5'$ and $3'$ ends of a

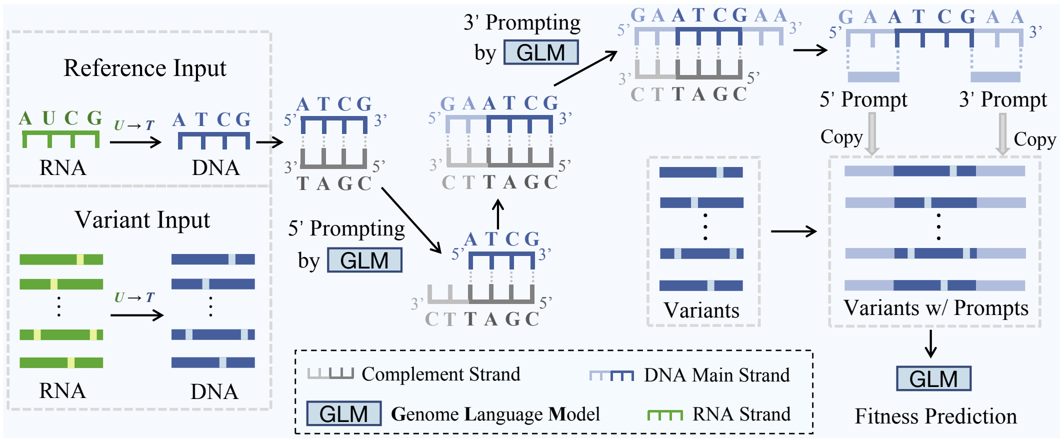

Figure 3: Workflow of BasePrompt for the RNA fitness prediction task. It first converts all input RNA sequences to DNA, replacing U with T. Then, operating solely on the reference DNA sequence, BasePrompt utilizes the complementary strand to perform upstream $5'$ and downstream $3'$ prompting autoregressively by a Genome Language Model (GLM). Generated prompts are then concatenated to the respective $5'$ and $3'$ ends of each variant sequence, creating a full set of prompted variants. Finally, these prompted sequences are fed into the same GLM for fitness prediction.

DNA strand, defined by their distinct chemical termini, determine the direction of synthesis. During processes such as DNA replication and transcription, new nucleotides are exclusively added to the $3'$ terminus, thereby extending the chain in a unidirectional $5'$ to $3'$ manner.

For autoregressive generation, the model predicts the next nucleotide token x_{t+1} conditioned on the sequence $x_1, x_2, \ldots, x_t$, formally expressed in Equation (1).

$$P(x_{t+1} \mid x_1, x_2, \ldots, x_t) = \text{softmax}(f(x_1, x_2, \ldots, x_t)) \tag{1}$$

Here, $f(\cdot)$ is a function, typically implemented by a genome language model, that maps the sequence $x_1, x_2, \ldots, x_t$ to logits over the next possible nucleotide token. The softmax function normalizes these outputs into valid probabilities. This process continues iteratively to generate the full sequence.

3.3 Reverse Complement and Prompting

We propose that the inherent symmetry of DNA, with its double-stranded structure, may help overcome the prompting direction challenge. In addition to the main strand of DNA, there exists a complementary reverse strand, oriented in the opposite direction ($5'$ to $3'$ opposite to $3'$ to $5'$) of the main strand. This complementary and reverse structure offers an opportunity to extend the context for sequence generation by utilizing the reverse complement strand.

Let $x_1, x_2, \ldots, x_t$ represent the nucleotide sequence of the main strand, from $5'$ to $3'$. The corresponding reverse complement sequence is denoted as $\hat{x}_t, \hat{x}_{t-1}, \ldots, \hat{x}_1$. For example, if x_i is the nucleotide at position i in the main strand, then $\hat{x}_{t-i}$ is the complementary base in the reverse strand at the corresponding position, as shown in Figure 4 (contents in black color).

By transforming to the reverse complement, we enable predictions for the downstream sequence ($3'$) on the reverse complement strand, which corresponds to the upstream ($5'$) sequence on the main strand. Specifically, the prediction on the reverse complement is $P(\hat{x}_{t+1} \mid x_t, x_{t-1}, \ldots, x_1)$. This allows us to predict the *nonexistent* context on the main strand shown in the contents in blue of Figure 4. We assume that the token before x_1 is x_{-1}, indicating that x_0 does not exist.

After generating the downstream of the reverse complement strand, we can map the generated bases to the main strand. Such a newly generated part is actually the upstream prompt of the main strand. Detailed steps are shown in the Section C. We formalize such a process in Equation (2).

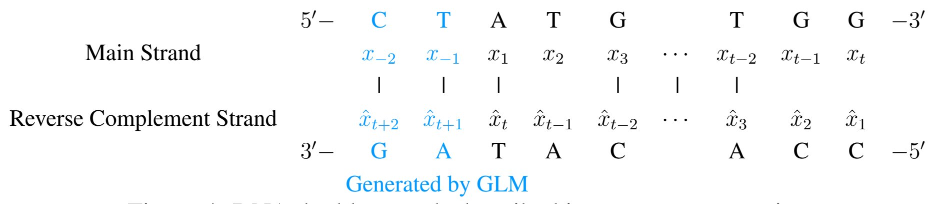
5′– C T A T G T G G –3′
Main Strand
x_{-2} x_{-1} x_1 x_2 x_3 $\cdots$ x_{t-2} x_{t-1} x_t
Reverse Complement Strand
$\hat{x}_{t+2}$ $\hat{x}_{t+1}$ $\hat{x}_t$ $\hat{x}_{t-1}$ $\hat{x}_{t-2}$ $\cdots$ $\hat{x}_3$ $\hat{x}_2$ $\hat{x}_1$
3′– G A T A C A C C –5′
Generated by GLM
Figure 4: DNA double strands described in sequence generation.

$$\begin{aligned} P(x_{-1} \mid x_t, x_{t-1}, \ldots, x_1) &= \text{compl}(P(\hat{x}_{t+1} \mid x_t, x_{t-1}, \ldots, x_1) \\ &= \text{compl}(\text{softmax}(f(\hat{x}_1, \hat{x}_2, \ldots, \hat{x}_t))) \end{aligned} \tag{2}$$

The compl$(\cdot)$ represents the probability of the complementary bases, and the function $f(\cdot)$ here is the same as in Equation (1), as genome language models are pre-trained on both strands [11, 41, 49]. By incorporating the reverse complement strand, we can effectively generate bidirectional prompts. Let N denote the number of tokens of the prompt, and we can now formalize generation as shown in Equation (3).

$$P(x_{t+1} \mid x_{-N}, x_{-(N-1)}, \ldots, x_{-1}, x_1, x_2, \ldots, x_t) \tag{3}$$

According to the introduction above, we can now leverage the DNA symmetry to generate upstream prompts during inference by sampling on the next-nucleotide probability. Notably, this symmetry is bidirectional, meaning we can start from the reverse complement strand and, by reversing the process, operate again on the main strand. More details can be found in Section C.

4 Experiment

To evaluate the effectiveness of BasePrompt, we conduct experiments in a zero-shot setting and utilize only the model inference without any tuning.

4.1 Experimental Settings

We introduce the tasks, datasets, models, and baselines as follows. The detailed information of our four datasets is depicted in Table 1. Further experimental details are provided in Section B.

Task-A (main): RNA fitness prediction. We evaluate BasePrompt by predicting the functional effect of RNA sequences in a zero-shot manner on the RNAGym benchmark [4]. It comprises 70 DMS assays, covering over one million variants across diverse RNA types and species, with sequence lengths ranging from 45 to 5,592 bases. We employ four metrics: Spearman's rank correlation (Spearman), Area Under the Receiver Operating Characteristic Curve (AUC), Matthews Correlation Coefficient (MCC), and Area Under the Precision-Recall Curve (AUPRC).

Task-B (auxiliary): DNA fitness prediction. We take the ClinVar dataset [26] to compare BasePrompt with the native prompt from the genome. The task is predicting the pathogenicity of human clinical single-nucleotide variants. For ClinVar, we adopt the version from [9][2], which contains 40,976 samples. Our metrics include Spearman and AUPRC.

Task-C (auxiliary): DNA next-base prediction. Since DNA has the "ground truth" prompt which RNA does not have, we further evaluate the synthetic prompt of BasePrompt on the DNA next-base prediction task [49][3], which is then filtered to retain sequences containing only A, G, C, and T. The task requires the model to predict the next N bases given an input DNA sequence. We evaluate generation quality using three metrics that capture different aspects of performance. (1) Accuracy: The percentage of correctly predicted bases, calculated as $(N_{correct}/N) \times 100\%$. (2) GC Content

[2]https://huggingface.co/datasets/songlab/clinvar

[3]https://huggingface.co/datasets/GenerTeam/next-kmer-prediction

Table 1: Information about our datasets. RNAGym serves as the main dataset for evaluation, while ClinVar and the next k-base prediction (NBP) are used as auxiliary datasets for analysis.

Dataset	Modality	Task	Species	Size
RNAGym	RNA	Fitness Prediction	Eukaryote, Prokaryote, Virus	1,117,995
ClinVar	DNA	Fitness Prediction	Human	40,976
NBP	DNA	Generation	Eukaryote, Prokaryote, Virus	84,648

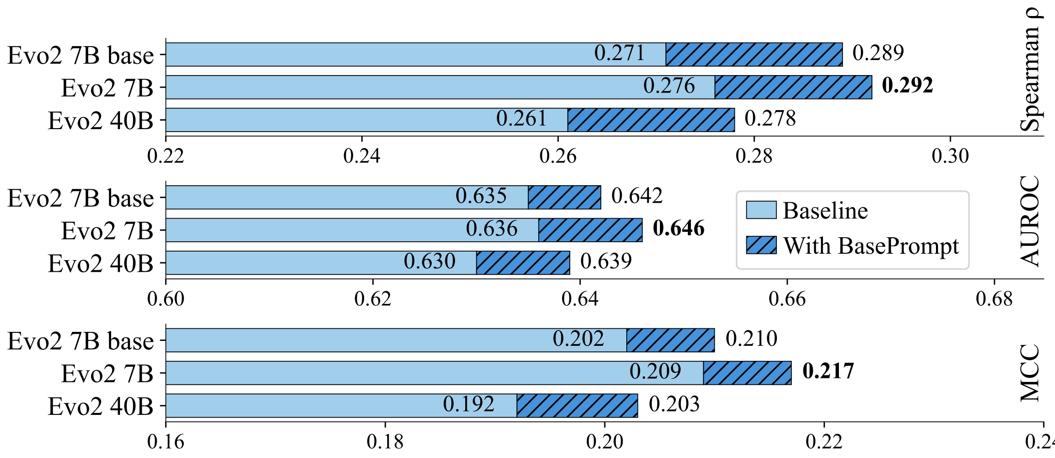

Figure 5: BasePrompt improves performance across diverse models on the RNAGym benchmark. We evaluate our method on the Evo families with the same prompt length of three. Bold numbers highlight the best performance.

Difference: The absolute difference between the GC ratio of the generated bases and the ground-truth bases averaged on all samples. (3) K-mer Jensen-Shannon Divergence (JSD): The JSD between the k-mer frequency distributions of the generated and ground-truth sequences.

Model and sampling. We conduct experiments using recently released genome language models (GLMs) to ensure a comprehensive evaluation across different architectures and scales. Specifically, we employ five models in RNA fitness prediction: Evo1 [36], Evo1.5 [34], and Evo2 [11] (7B base, 7B, 40B). For Evo models, which use single-nucleotide tokenization, we restrict generation to the four valid DNA bases and set top-k=1, *i.e.*, greedy strategy. In DNA tasks, we also include the GENERator [49] models (1.2B, 3B), which use 6-mer tokenization. We set sampling hyperparameters as temperature=1.0, top-k=4, and top-p=1.0. The same GLM is used for both prompting and performing the downstream task.

4.2 BasePrompt Improves RNA Fitness Prediction

For RNA fitness prediction, Genome Language Models (GLMs) compute the negative log-likelihood of the entire sequence S, and the length-normalized average serves as the predicted fitness score $f(S)$ [11]. An ensemble score, $(f(S) + f(S_{rc}))/2$, can be obtained by averaging with the reverse complement, S_{rc}. In the official RNAGym benchmark, different models were inconsistently reported—Evo1.5 with direct prediction and Evo2-7B with RC ensemble. Since we observed that RC ensembling has a non-trivial effect, we re-implemented all baselines and reported ensemble results for fair comparison. We report the ensembled results in the main text, and the direct predictions are provided in Section D.

BasePrompt achieves state-of-the-art performance on RNAGym. Our method brings consistent improvement across three metrics on the Evo series, as illustrated in Figure 5. We utilize a prompt length of three for these models. The performance of additional baseline models is sourced from the RNAGym paper [4], including Nucleotide Transformer (NT) [17], RiNALMo [38], RNA-FM [15],

Table 2: BasePrompt improves performance across diverse models and achieves SOTA results on the RNAGym benchmark. Our method achieves relative improvements of 6.0–16.4% in Spearman ρ, 1.2–3.9% in AUROC, and 4.0–24.3% in MCC over the respective baseline models. We use the reverse complement ensemble for both baselines and ours. Gray rows indicate our results, while bold numbers denote the best performance. Results of each model's best prompt length are reported.

Model Name	Spearman $\rho \uparrow$	AUROC $\uparrow$	MCC $\uparrow$
RNA-FM	0.217	0.605	0.155
RNAErnie	0.189	0.598	0.154
NT	0.163	0.577	0.115
RiNALMo	0.155	0.582	0.122
GenSLM	0.122	0.558	0.083
Evo1	0.192	0.590	0.131
w/ BasePrompt	0.211	0.604	0.146
Evo1.5	0.199	0.594	0.147
w/ BasePrompt	0.232	0.617	0.183
Evo2 7B base	0.271	0.635	0.202
w/ BasePrompt	0.289	0.643	**0.219**
Evo2 7B	0.276	0.636	0.209
w/ BasePrompt	**0.292**	**0.646**	0.217
Evo2 40B	0.261	0.630	0.192
w/ BasePrompt	0.288	0.645	0.212

Table 3: BasePrompt consistently outperforms the baseline in RNAGym across diverse sampling hyperparameters, achieving relative improvements ranging from 1.6% to 7.2% in Spearman's rank correlation. All experiments are conducted using the Evo2 7B with a prompt length of three.

Top-k	Top-p	Spearman ρ	AUROC	MCC
Baseline		0.276	0.636	0.209
1	-	0.292	0.646	0.217
2	-	0.296	0.648	0.223
3	-	0.295	0.648	0.221
4	-	0.280	0.641	0.207
-	0.3	0.282	0.641	0.211
-	0.5	0.296	0.648	0.222
-	0.7	0.282	0.641	0.211
-	0.9	0.272	0.637	0.209

RNAernie [45], and GenSLM [54]. Among these, BasePrompt on Evo2 7B achieves the highest performance, with a relative improvement of 6% in Spearman's rank correlation.

BasePrompt performs even better with more flexible prompt lengths. In previous experiments, we reported the result of a fixed length of three for consistency, as shown in Figure 5. However, BasePrompt can be more powerful when equipped with a selective length for each model. As illustrated in Table 2, our method achieves relative improvements of 6.0–16.4% in Spearman ρ, 1.2–3.9% in AUROC, and 4.0–24.3% in MCC over the respective baseline models. It demonstrates the generality and potential of our method. The prompt lengths of BasePrompt for models on the table from top to bottom are 32, 32, 5, 3, and 5.

BasePrompt is robust to sampling hyper-parameters of GLM generation. Our method consistently outperforms the baseline across various top-k and top-p values, as shown in Table 3. We use greedy sampling (top-$k = 1$) in the main experiment for controlled comparison without randomness

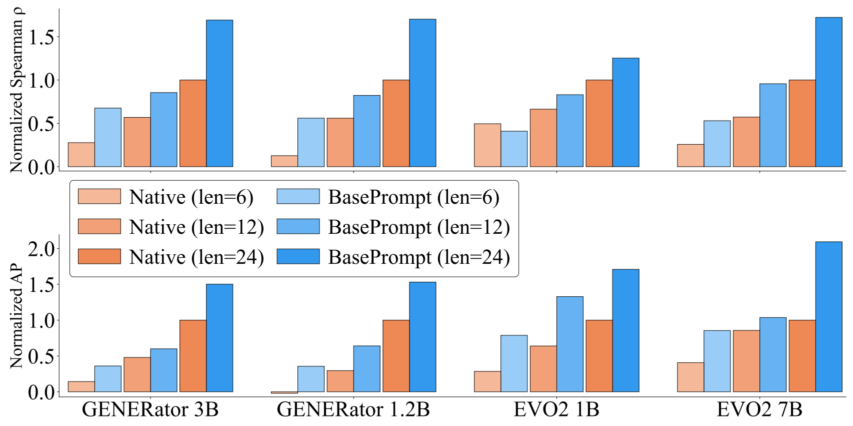

Figure 6: BasePrompt outperforms the native genome prompt on the ClinVar dataset under limited expansion. The "len" denotes the prompt length. For fair comparison, we normalize Spearman's rank correlation (Spearman ρ) and average precision (AP) by setting the value at input length 510 (prompt length=0) to 0.0, and the value at prompt length of 24 to 1.0.

and get a Spearman's ρ of 0.287 on Evo2 7B. However, the top-$k = 2$ brings a better Spearman's ρ of 0.297. It demonstrates the hidden potential of our BasePrompt.

BasePrompt is computationally efficient for large-scale fitness prediction. We only generate a sequence with three bases 70 times, a negligible computational overhead when compared to the 1,117,995 model inferences required for fitness prediction across all variants. Additionally, the extra 6 bases (3+3) introduced by our prompt contribute only 1.5% to the overall computational cost of fitness prediction, which is derived by averaging the number and length of sequences for each assay.

4.3 Auxiliary Experiments on DNA for Analysis

To further analyze BasePrompt, we turn to DNA-based tasks where the genome could provide natural prompts. We concentrate on the performance of discriminative and generative tasks, but not interpretable motifs, since the prompt is used for steering downstream GLMs but not for humans.

4.3.1 BasePrompt Aids Clinical Variant Effect Prediction

On the ClinVar dataset [26], the model is given a variant-containing sequence and a matched reference, and must classify the variant as pathogenic or benign in a zero-shot setting. Following Evo2's setup [11][4], the variant effect is measured by the log-likelihood difference between the mutant and reference. For comparison, we consider three inputs: (i) the original sequence S_{origin}, (ii) native prompt with real genomic prompt, $S_{5'\text{native}} + S_{\text{origin}} + S_{3'\text{native}}$, and (iii) prompt generated by our BasePrompt, $S_{5'\text{our}} + S_{\text{origin}} + S_{3'\text{our}}$.

BasePrompt outperforms native genomic prompt under short prompts. As shown in Figure 6, orange bars represent native prompt ($S_{5'\text{native}} + S_{\text{origin}} + S_{3'\text{native}}$) and blue bars represent BasePrompt ($S_{5'\text{our}} + S_{\text{origin}} + S_{3'\text{our}}$). For comparability, we normalize Spearman's rank correlation and average precision by setting the score at no prompting(S_{origin}) to 0.0 and the score at a prompt length of 24 per side ($S_{5'\text{native}} + S_{\text{origin}} + S_{3'\text{native}}$) to 1.0. Notably, our generated prompts consistently outperform native prompts when the prompt length is less than or equal to 24 bases on each side.

We hypothesize that GLMs, through large-scale pretraining with next-token prediction, acquire the ability to reconstruct "efficient" contextual signals. In contrast, a native prompt may contain redundant information. Since the same GLM serves as both prompt generator and predictor, the synthesized prompt may have bridged the distributional gap closer to the model's pretraining distribution.

[4]The public source code in Github can be found here.

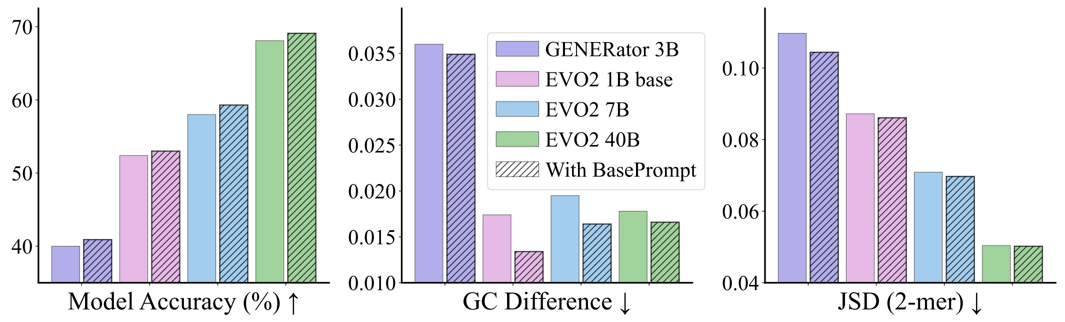

Figure 7: The bases predicted by BasePrompt show a closer alignment with the genome. Bold numbers represent our performance, while the regular numbers correspond to the raw input results. BasePrompt yields a higher accuracy, lower GC difference, and 2-mer Jensen-Shannon Divergence.

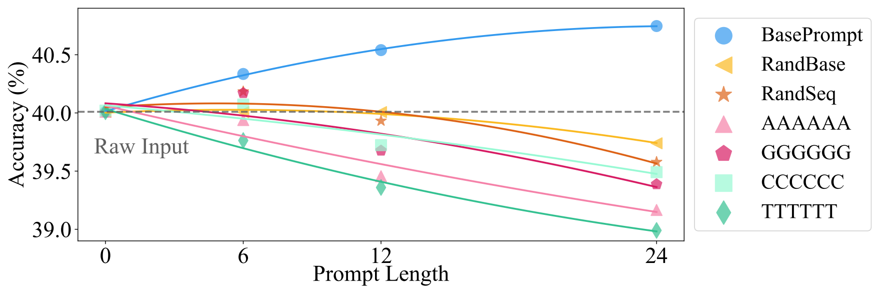

Figure 8: BasePrompt indicates generating a positively meaningful prompt, rather than just random expansion. The task is to predict the next 6 bases given a sequence of length 192.

4.3.2 Assessing the Biological Plausibility of Generated Prompts

It is also necessary to evaluate whether the generated sequences remain biologically plausible. We adopt the dataset from Wu et al. [49] and then restricts it to canonical nucleotides (A, T, C, G). We ask GLMs to predict the next k bases prediction, conditioned on a 192-base input sequence.

BasePrompt yields generations closely aligned with biologically plausible patterns. As shown in Figure 7, our method consistently achieves higher base-level accuracy and smaller GC-content difference compared to direct prediction on raw input, even under the $5'$ prompt of 192 bases beyond the original input. Furthermore, the 2-mer JSD remains lower across species groups, indicating that the generated prompt better preserves local sequence statistics. Additional results for varying prompt lengths, input lengths, GLMs, and sampling strategies are provided in Section E.

BasePrompt generates more informative prompts compared to other prompting strategies. We compare the performance of BasePrompt with various prompting approaches in Figure 8. The RandomSeq is to randomly generate a sequence and prepend it to the original input. We modify this prompting by selecting the bases from the original sequence, *i.e.*, the RandomSeq strategy. Additionally, we explore fixed-sequence prompts, such as repeating A/G/C/T.

5 Conclusion

We present BasePrompt, a novel framework that leverages Genome Language Models (GLMs) to generate bidirectional RNA prompts, enhancing performance in downstream tasks without requiring domain-specific fine-tuning. By enabling GLMs to write their own prompts, we close a critical gap in the application of prompting to RNA sequences. Our method achieves state-of-the-art results in RNA fitness prediction and demonstrates robustness across multiple GLM models. Additionally, we show that the generated prompts are efficient and effective, offering consistent improvements in various genomic tasks. BasePrompt represents a significant step toward unlocking the full potential of GLMs.

References

[1] Rishabh Agarwal, Avi Singh, Lei Zhang, Bernd Bohnet, Luis Rosias, Stephanie Chan, Biao Zhang, Ankesh Anand, Zaheer Abbas, Azade Nova, et al. Many-shot in-context learning. *Advances in Neural Information Processing Systems*, 37:76930–76966, 2024.

[2] Khaled Alomar, Halil Ibrahim Aysel, and Xiaohao Cai. Data augmentation in classification and segmentation: A survey and new strategies. *Journal of Imaging*, 9(2):46, 2023.

[3] Weizhi An, Yuzhi Guo, Yatao Bian, Hehuan Ma, Jinyu Yang, Chunyuan Li, and Junzhou Huang. Modna: motif-oriented pre-training for dna language model. In *Proceedings of the 13th ACM international conference on bioinformatics, computational biology and health informatics*, pages 1–5, 2022.

[4] Rohit Arora, Murphy Angelo, Christian Andrew Choe, Courtney A Shearer, Aaron W Kollasch, Fiona Qu, Ruben Weitzman, Artem Gazizov, Sarah Gurev, Erik Xie, et al. Rnagym: Large-scale benchmarks for rna fitness and structure prediction. *bioRxiv*, pages 2025–06, 2025.

[5] Hyojin Bahng, Ali Jahanian, Swami Sankaranarayanan, and Phillip Isola. Exploring visual prompts for adapting large-scale models. *arXiv preprint arXiv:2203.17274*, 2022.

[6] Jakub M Bartoszewicz, Anja Seidel, Robert Rentzsch, and Bernhard Y Renard. Deepac: predicting pathogenic potential of novel dna with reverse-complement neural networks. *Bioinformatics*, 36(1):81–89, 2020.

[7] Markus Bayer, Marc-André Kaufhold, and Christian Reuter. A survey on data augmentation for text classification. *ACM Computing Surveys*, 55(7):1–39, 2022.

[8] Gonzalo Benegas, Sanjit Singh Batra, and Yun S Song. Dna language models are powerful predictors of genome-wide variant effects. *Proceedings of the National Academy of Sciences*, 120(44):e2311219120, 2023.

[9] Gonzalo Benegas, Carlos Albors, Alan J Aw, Chengzhong Ye, and Yun S Song. A dna language model based on multispecies alignment predicts the effects of genome-wide variants. *Nature Biotechnology*, pages 1–6, 2025.

[10] Gonzalo Benegas, Chengzhong Ye, Carlos Albors, Jianan Canal Li, and Yun S Song. Genomic language models: opportunities and challenges. *Trends in Genetics*, 2025.

[11] Garyk Brixi, Matthew G Durrant, Jerome Ku, Michael Poli, Greg Brockman, Daniel Chang, Gabriel A Gonzalez, Samuel H King, David B Li, Aditi T Merchant, et al. Genome modeling and design across all domains of life with evo 2. *bioRxiv*, pages 2025–02, 2025.

[12] Richard C Brown and Gerton Lunter. An equivariant bayesian convolutional network predicts recombination hotspots and accurately resolves binding motifs. *Bioinformatics*, 35(13):2177–2184, 2019.

[13] Tom Brown, Benjamin Mann, Nick Ryder, Melanie Subbiah, Jared D Kaplan, Prafulla Dhariwal, Arvind Neelakantan, Pranav Shyam, Girish Sastry, Amanda Askell, et al. Language models are few-shot learners. *Advances in neural information processing systems*, 33:1877–1901, 2020.

[14] Zhen Cao and Shihua Zhang. Simple tricks of convolutional neural network architectures improve dna–protein binding prediction. *Bioinformatics*, 35(11):1837–1843, 2019.

[15] Jiayang Chen, Zhihang Hu, Siqi Sun, Qingxiong Tan, Yixuan Wang, Qinze Yu, Licheng Zong, Liang Hong, Jin Xiao, Tao Shen, et al. Interpretable rna foundation model from unannotated data for highly accurate rna structure and function predictions. *arXiv preprint arXiv:2204.00300*, 2022.

[16] Jim Clauwaert and Willem Waegeman. Novel transformer networks for improved sequence labeling in genomics. *IEEE/ACM Transactions on Computational Biology and Bioinformatics*, 19(1):97–106, 2020.

[17] Hugo Dalla-Torre, Liam Gonzalez, Javier Mendoza-Revilla, Nicolas Lopez Carranza, Adam Henryk Grzywaczewski, Francesco Oteri, Christian Dallago, Evan Trop, Bernardo P de Almeida, Hassan Sirelkhatim, et al. Nucleotide transformer: building and evaluating robust foundation models for human genomics. *Nature Methods*, 22(2):287–297, 2025.

[18] Bernardo P de Almeida, Franziska Reiter, Michaela Pagani, and Alexander Stark. Deepstarr predicts enhancer activity from dna sequence and enables the de novo design of synthetic enhancers. *Nature genetics*, 54(5):613–624, 2022.

[19] Andrew G Duncan, Jennifer A Mitchell, and Alan M Moses. Improving the performance of supervised deep learning for regulatory genomics using phylogenetic augmentation. *Bioinformatics*, 40(4):btae190, 2024.

[20] Sin-Hang Fung, Zhenghao Zhang, Ran Wang, Chen Miao, Brian Shing-Hei Wong, Kelly Yichen Li, Chenyang Hong, Jingying Zhou, Kevin Y Yip, Stephen Kwok-Wing Tsui, et al. Few-shot in-context learning with large language models for antibody characterization. *bioRxiv*, pages 2025–02, 2025.

[21] Menglin Jia, Luming Tang, Bor-Chun Chen, Claire Cardie, Serge Belongie, Bharath Hariharan, and Ser-Nam Lim. Visual prompt tuning. In *European conference on computer vision*, pages 709–727. Springer, 2022.

[22] Jiyue Jiang, Zikang Wang, Yuheng Shan, Heyan Chai, Jiayi Li, Zixian Ma, Xinrui Zhang, and Yu Li. Biological sequence with language model prompting: A survey. *arXiv preprint arXiv:2503.04135*, 2025.

[23] Pranav Kantroo, Günter P Wagner, and Benjamin B Machta. In-context learning can distort the relationship between sequence likelihoods and biological fitness. *arXiv preprint arXiv:2504.17068*, 2025.

[24] David R Kelley, Jasper Snoek, and John L Rinn. Basset: learning the regulatory code of the accessible genome with deep convolutional neural networks. *Genome research*, 26(7):990–999, 2016.

[25] Takeshi Kojima, Shixiang Shane Gu, Machel Reid, Yutaka Matsuo, and Yusuke Iwasawa. Large language models are zero-shot reasoners. *Advances in neural information processing systems*, 35:22199–22213, 2022.

[26] Melissa J Landrum, Shanmuga Chitipiralla, Garth R Brown, Chao Chen, Baoshan Gu, Jennifer Hart, Douglas Hoffman, Wonhee Jang, Kuljeet Kaur, Chunlei Liu, et al. Clinvar: improvements to accessing data. *Nucleic acids research*, 48(D1):D835–D844, 2020.

[27] Nicholas Keone Lee, Ziqi Tang, Shushan Toneyan, and Peter K Koo. Evoaug: improving generalization and interpretability of genomic deep neural networks with evolution-inspired data augmentations. *Genome Biology*, 24(1):105, 2023.

[28] Jiahao Li, Zhourun Wu, Wenhao Lin, Jiawei Luo, Jun Zhang, Qingcai Chen, and Junjie Chen. ienhancer-elm: improve enhancer identification by extracting position-related multiscale contextual information based on enhancer language models. *Bioinformatics Advances*, 3(1): vbad043, 2023.

[29] Jiajia Liu, Mengyuan Yang, Yankai Yu, Haixia Xu, Kang Li, and Xiaobo Zhou. Large language models in bioinformatics: applications and perspectives. *arXiv preprint arXiv:2401.04155*, 2024.

[30] Vincent Mallet and Jean-Philippe Vert. Reverse-complement equivariant networks for dna sequences. *Advances in neural information processing systems*, 34:13511–13523, 2021.

[31] Haitao Mao, Guangliang Liu, Yao Ma, Rongrong Wang, Kristen Johnson, and Jiliang Tang. A survey to recent progress towards understanding in-context learning. *arXiv preprint arXiv:2402.02212*, 2024.

[32] Guillaume Marçais, C_S Elder, and Carl Kingsford. k-nonical space: sketching with reverse complements. *Bioinformatics*, 40(11):btae629, 2024.

[33] Joshua Meier, Roshan Rao, Robert Verkuil, Jason Liu, Tom Sercu, and Alex Rives. Language models enable zero-shot prediction of the effects of mutations on protein function. *Advances in neural information processing systems*, 34:29287–29303, 2021.

[34] Aditi T Merchant, Samuel H King, Eric Nguyen, and Brian L Hie. Semantic mining of functional de novo genes from a genomic language model. *bioRxiv*, 2024. doi: 10.1101/2024.12.17.628962. URL `https://www.biorxiv.org/content/early/2024/12/18/2024.12.17.628962`.

[35] Eric Nguyen, Michael Poli, Marjan Faizi, Armin Thomas, Michael Wornow, Callum Birch-Sykes, Stefano Massaroli, Aman Patel, Clayton Rabideau, Yoshua Bengio, et al. Hyenadna: Long-range genomic sequence modeling at single nucleotide resolution. *Advances in neural information processing systems*, 36:43177–43201, 2023.

[36] Eric Nguyen, Michael Poli, Matthew G. Durrant, Brian Kang, Dhruva Katrekar, David B. Li, Liam J. Bartie, Armin W. Thomas, Samuel H. King, Garyk Brixi, Jeremy Sullivan, Madelena Y. Ng, Ashley Lewis, Aaron Lou, Stefano Ermon, Stephen A. Baccus, Tina Hernandez-Boussard, Christopher Ré, Patrick D. Hsu, and Brian L. Hie. Sequence modeling and design from molecular to genome scale with evo. *Science*, 386(6723):eado9336, 2024. doi: 10.1126/science.ado9336. URL `https://www.science.org/doi/abs/10.1126/science.ado9336`.

[37] OpenAI. Introducing GPT-5. `https://openai.com/index/introducing-gpt-5`, 08 2025.

[38] Rafael Josip Penić, Tin Vlašić, Roland G Huber, Yue Wan, and Mile Šikić. Rinalmo: General-purpose rna language models can generalize well on structure prediction tasks. *Nature Communications*, 16(1):5671, 2025.

[39] Daniel Quang and Xiaohui Xie. Factornet: a deep learning framework for predicting cell type specific transcription factor binding from nucleotide-resolution sequential data. *Methods*, 166: 40–47, 2019.

[40] Melissa Sanabria, Jonas Hirsch, Pierre M Joubert, and Anna R Poetsch. Dna language model grover learns sequence context in the human genome. *Nature Machine Intelligence*, 6(8): 911–923, 2024.

[41] Yair Schiff, Chia-Hsiang Kao, Aaron Gokaslan, Tri Dao, Albert Gu, and Volodymyr Kuleshov. Caduceus: Bi-directional equivariant long-range dna sequence modeling. *arXiv preprint arXiv:2403.03234*, 2024.

[42] Avanti Shrikumar, Peyton Greenside, and Anshul Kundaje. Reverse-complement parameter sharing improves deep learning models for genomics. *BioRxiv*, page 103663, 2017.

[43] Howard M Temin and S Mizutami. Rna-dependent dna polymerase in virions of rous sarcoma virus., 1970.

[44] Shushan Toneyan, Ziqi Tang, and Peter K Koo. Evaluating deep learning for predicting epigenomic profiles. *Nature machine intelligence*, 4(12):1088–1100, 2022.

[45] Ning Wang, Jiang Bian, Yuchen Li, Xuhong Li, Shahid Mumtaz, Linghe Kong, and Haoyi Xiong. Multi-purpose rna language modelling with motif-aware pretraining and type-guided fine-tuning. *Nature Machine Intelligence*, 6(5):548–557, 2024.

[46] Zaitian Wang, Pengfei Wang, Kunpeng Liu, Pengyang Wang, Yanjie Fu, Chang-Tien Lu, Charu C Aggarwal, Jian Pei, and Yuanchun Zhou. A comprehensive survey on data augmentation. *arXiv preprint arXiv:2405.09591*, 2024.

[47] Zeyuan Wang, Binbin Chen, Keyan Ding, Jiawen Cao, Ming Qin, Yadan Niu, Xiang Zhuang, Xiaotong Li, Kehua Feng, Tong Xu, et al. Multi-purpose controllable protein generation via prompted language models. *bioRxiv*, pages 2024–11, 2024.

[48] James D Watson and Francis HC Crick. Molecular structure of nucleic acids: a structure for deoxyribose nucleic acid. *Nature*, 171(4356):737–738, 1953.

[49] Wei Wu, Qiuyi Li, Mingyang Li, Kun Fu, Fuli Feng, Jieping Ye, Hui Xiong, and Zheng Wang. Generator: A long-context generative genomic foundation model. *arXiv preprint arXiv:2502.07272*, 2025.

[50] Suorong Yang, Weikang Xiao, Mengchen Zhang, Suhan Guo, Jian Zhao, and Furao Shen. Image data augmentation for deep learning: A survey. *arXiv preprint arXiv:2204.08610*, 2022.

[51] Hannah Zhou, Avanti Shrikumar, and Anshul Kundaje. Benchmarking reverse-complement strategies for deep learning models in genomics. *bioRxiv*, pages 2020–11, 2020.

[52] Hannah Zhou, Avanti Shrikumar, and Anshul Kundaje. Towards a better understanding of reverse-complement equivariance for deep learning models in genomics. In *Machine Learning in Computational Biology*, pages 1–33. PMLR, 2022.

[53] Jian Zhou and Olga G Troyanskaya. Predicting effects of noncoding variants with deep learning–based sequence model. *Nature methods*, 12(10):931–934, 2015.

[54] Maxim Zvyagin, Alexander Brace, Kyle Hippe, Yuntian Deng, Bin Zhang, Cindy Orozco Bohorquez, Austin Clyde, Bharat Kale, Danilo Perez-Rivera, Heng Ma, et al. Genslms: Genome-scale language models reveal sars-cov-2 evolutionary dynamics. *The International Journal of High Performance Computing Applications*, 37(6):683–705, 2023.

Appendix

In the appendix, we first discuss the use of Large Language Models (LLMs) in Section A. We then detail the experimental settings in Section B. Next, we provide an in-depth description of the BasePrompt process in Section C. Additionally, we present supplementary experiments related to RNA and DNA in Section D and Section E, respectively.

A The Use of Large Language Models

In the process of writing this paper, large language models (LLMs) played a significant role in supporting various tasks. Specifically, GPT-5 [37] was used to assist with grammar checking and error correction, refining wording and phrasing, and providing suggestions for visualizations of tables and figures. These tools were employed to enhance the clarity, coherence, and presentation of the content. The LLMs were primarily used for tasks that involved improving the linguistic quality of the text and offering guidance on the effective visualization of data, but they did not contribute to the scientific ideation or the formulation of research hypotheses. The contributions of these models are acknowledged to ensure transparency in the research process.

B Experimental Settings

All experiments are conducted in a zero-shot setting, utilizing only the inference capabilities of pre-trained models without any fine-tuning. We design a comprehensive suite of four tasks to evaluate BasePrompt across both generative and discriminative capabilities on DNA and RNA sequences. The tasks are detailed in Sections B.1 to B.3. We then describe the models and hyperparameters in Section B.4 and elaborate on the core zero-shot mechanism for variant effect prediction in Section B.5.

B.1 Task-A: RNA Variant Effect Prediction on RNAGym

Task and Dataset We evaluate BasePrompt on the RNA variant effect prediction (VEP) task using the RNAGym benchmark [4]. The objective is to predict the functional effect of RNA sequence variants in a zero-shot manner. Performance is evaluated by comparing the predicted functional ranking of variants against experimental measurements from deep mutational scanning (DMS) assays. The benchmark comprises 70 standardized DMS assays, covering 1,117,995 variants across diverse RNA types (*e.g.*, mRNA-splicing, tRNA, aptamer, ribozyme) and species (eukaryote, prokaryote, virus, human), with sequence lengths ranging from 45 to 5,592 bases.

Evaluation and Metrics We employ four complementary metrics. Spearman's rank correlation assesses the monotonic relationship between predicted scores and experimental measurements. Area Under the Receiver Operating Characteristic Curve (AUC) evaluates the model's ability to discriminate between functional and non-functional variants. Matthews Correlation Coefficient (MCC) provides a balanced measure of classification quality, even for imbalanced datasets. Area Under the Precision-Recall Curve (AUPRC) is particularly informative for imbalanced data, focusing on the performance of identifying positive instances. To ensure a balanced evaluation across RNA types with varying numbers of assays, we first compute the average performance for each RNA type and then report the mean of these per-type averages.

B.2 Task-B: Next-base Prediction

Task and Dataset We assess the generative capabilities of models on a DNA next-base prediction task, using data from various species, including eukaryote, prokaryote, virus, and human [49, 40]. The task requires the model to predict the next N bases given an input DNA sequence. We use the dataset from [49][5], filtered to retain only sequences containing A, G, C, and T, resulting in 84,648 sequences. Dataset statistics are provided in Table 5.

Evaluation and Metrics We evaluate generation quality using three metrics that capture different aspects of performance. (1) Accuracy: The percentage of correctly predicted bases, calculated as

[5]https://huggingface.co/datasets/GenerTeam/next-kmer-prediction

$(N_{correct}/N) \times 100\%$. (2) GC Content Difference: The absolute difference between the GC content ratio of the generated bases and the ground-truth bases. (3) k-mer Jensen-Shannon Divergence (JSD): The JSD between the k-mer frequency distributions of the generated and ground-truth sequences. These metrics provide a multi-grained analysis: accuracy measures base-level precision, GC content difference reflects compositional distribution, and k-mer JSD captures local sequence statistics.

B.3 Task-C: Clinical Variant Effect Prediction

We further evaluate BasePrompt on a discriminative task focused on predicting the pathogenicity of human clinical single-nucleotide variants (SNVs). We use the ClinVar dataset [26] to assess generalization on clinically significant variations. The model is given a pair of sequences—one containing the SNV and a corresponding reference—and must classify the variant as pathogenic or benign in a zero-shot setting. We adopt the version from [9][6], which contains 40,976 samples.

Evaluation and Metrics Our evaluation metrics include Spearman and AUPRC. Spearman's Rank Correlation quantifies the monotonic relationship between the model's predicted pathogenicity scores (*e.g.*, logits or probabilities) and the ground-truth binary labels. It assesses how well the model preserves the inherent ranking of variants by their severity, indicating if higher scores generally correspond to more severe variants. AUPRC is particularly informative for imbalanced datasets, such as clinical variant annotations, where pathogenic variants are often rarer. It focuses on the trade-off between precision and recall for the positive class (pathogenic variants), providing a more sensitive measure of performance when identifying these critical cases.

B.4 Models and Hyperparameters

We conduct experiments using recently released genome language models (GLMs) to ensure a comprehensive evaluation across different architectures and scales. Specifically, we employ six models from two families: GENERator-1.2B, GENERator-3B [49], Evo2-1B-base, Evo2-7B, Evo2-7B-base, and Evo2-40B [11]. For generative tasks, we employ standard sampling strategies: temperature, top-k, and top-p. Our default settings are chosen based on the models' tokenization schemes. For GENERator models, which use 6-mer tokenization, we set temperature=1.0, top-k=4, and top-p=1.0. For Evo2 models, which use single-nucleotide tokenization, we restrict generation to the four valid DNA bases (A, T, C, G) by setting top-k=1, effectively performing greedy decoding. The robustness of BasePrompt to variations in sampling strategies is further discussed and evaluated in Table 11.

BasePrompt is a pure inference-time approach that enhances model performance by generating the prompt, without altering the underlying model architecture or its downstream task pipeline. The specific application of BasePrompt to each task is detailed in Section C. For consistency and fair comparison, the same GLM is used for both generating the bidirectional prompts and for performing the final downstream task. For instance, if an experiment is labeled Evo2 7B, it signifies that Evo2 7B was leveraged for both prompting and the subsequent prediction.

B.5 Zero-shot Mechanism of Variant Effect Prediction

In this section, we introduce the detailed mechanism of zero-shot implementation on variant classification. In a zero-shot setting, the model is not explicitly trained on labeled variant effect data but instead leverages its pretrained knowledge of genomic sequences to assess mutation impact directly from sequence likelihoods. The input to the model consists of a pair of sequences: a reference sequence (ref) and a variant sequence (var), differing by a single nucleotide variant (SNV).

Here, the reference sequence $\mathbf{x}^{\text{ref}}$ represents the wild-type (non-mutated) version of a genomic region, while $\mathbf{x}^{\text{var}}$ is an otherwise identical sequence that contains an SNV at a specific position. The task is to predict whether the variant results in loss of function (LoF) or the opposite (Non-LOF). Given a reference sequence $\mathbf{x}^{\text{ref}}$ and a variant sequence $\mathbf{x}^{\text{var}}$, we compute a log-likelihood score for each sequence by averaging the model's log-probabilities over all positions:

[6]Dataset link.

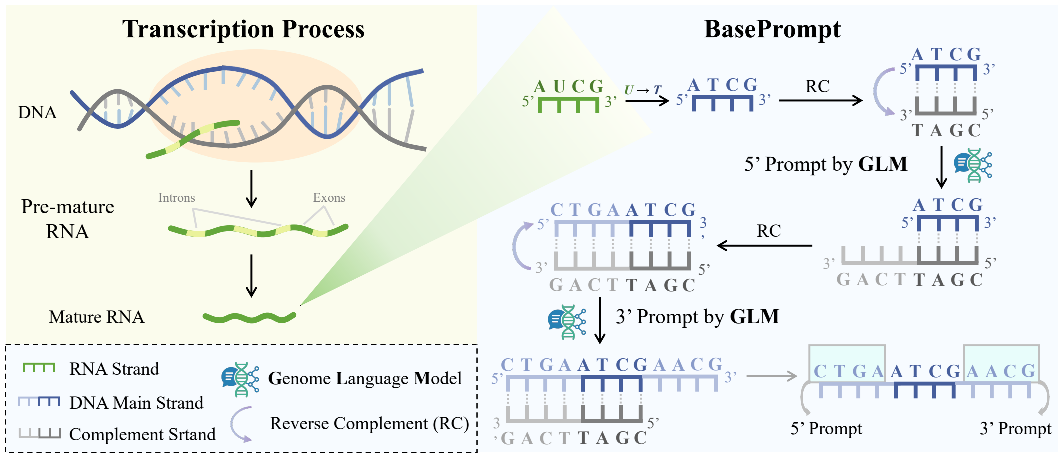

Figure 9: Motivation and illustration of BasePrompt. The transcription from DNA to RNA involves mechanisms such as alternative splicing, which can irreversibly limit the available sequence context. Inspired by the complementary double-helix structure of DNA, we introduce BasePrompt, a novel method for RNA prompting. It generates the bidirectional prompts by autoregressively predicting the upstream $5'$ and downstream $3'$ prompts directly on the main strand. Our method is inference-time and model-agnostic, making it both convenient and effective.

Figure 10: Input DNA sequence described in Markov chain.

	$5'-$	A	T	G		T	G	G	$-3'$
Main Stand		x_1	x_2	x_3	$\cdots$	x_{t-2}	x_{t-1}	x_t	

$$\log p(\mathbf{x}) = \frac{1}{L}\sum_{t=1}^{L}\log p(x_t \mid \mathbf{x}_{<t}) \tag{4}$$

Here, L is the sequence length, and $p(x_t \mid \mathbf{x}_{<t})$ is the probability assigned to the true nucleotide at position t under the model's autoregressive output. In practice, this is computed by applying a log-softmax over the model's output logits at each position and gathering the value corresponding to the ground-truth token. Then the delta likelihood score between the reference and variant is calculated as:

$$\Delta\mathcal{L} = \log p(\mathbf{x}^{\text{ref}}) - \log p(\mathbf{x}^{\text{var}}) \tag{5}$$

This score serves as a proxy for mutation impact, with higher values indicating greater disruption under the model's learned distribution. To evaluate the classification performance of this approach, the Area Under the Receiver Operating Characteristic (AUROC) is computed based on the delta likelihood score.

C BasePrompt Mechanism

We describe the detailed process involved in generating the DNA strands based on the Markov chain model outlined in the main text. The overview is illustrated in Figure 9. This process involves inputting an initial DNA sequence, generating the reverse complement strand, and mapping generated bases to the main strand using the principle of complementary base pairing. The methodology involves simulating both the main and reverse complement strands, as shown in Figure 10, Figure 11, Figure 12, and Figure 13.

For detailed application in generation and variant classification tasks, we describe the usage of BasePrompt in Figure 3. We define the expansion of the original $5' - \textit{sequence} \rightarrow 3'$ by GLM as $3'$ prompting, and the reverse complement of $5' \leftarrow \textit{sequence} - 3'$ by GLM as $5'$ prompting, details

Figure 11: DNA double strands described in a Markov chain.

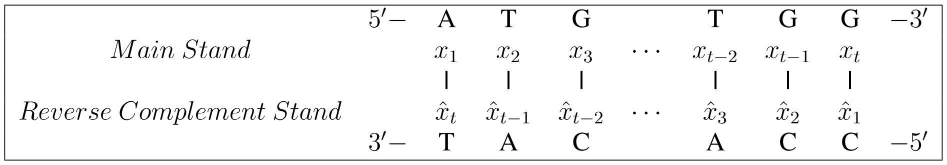

5′− A T G T G G −3′
Main Stand
x_1 x_2 x_3 $\cdots$ x_{t-2} x_{t-1} x_t
Reverse Complement Stand
$\hat{x}_t$ $\hat{x}_{t-1}$ $\hat{x}_{t-2}$ $\cdots$ $\hat{x}_3$ $\hat{x}_2$ $\hat{x}_1$
3′− T A C A C C −5′

Figure 12: Generating the downstream of the reverse complement strand.

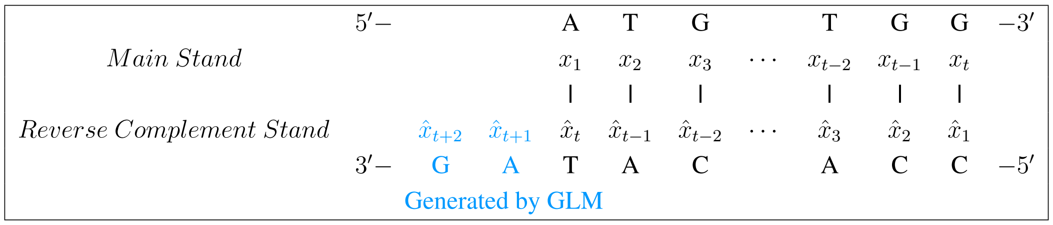

5′− A T G T G G −3′
Main Stand
x_1 x_2 x_3 $\cdots$ x_{t-2} x_{t-1} x_t
Reverse Complement Stand
$\hat{x}_{t+2}$ $\hat{x}_{t+1}$ $\hat{x}_t$ $\hat{x}_{t-1}$ $\hat{x}_{t-2}$ $\cdots$ $\hat{x}_3$ $\hat{x}_2$ $\hat{x}_1$
3′− G A T A C A C C −5′
Generated by GLM

of which are shown in Figure 3. The upper section illustrates the $5'$ prompting for the generative task. Additionally, further inference can facilitate the formulation of a bidirectional prompting. The lower section depicts the variant classification process, where both the $5' + 3'$ prompts are applied to the reference sequence. These prompts are then concatenated to the respective $5'$ and $3'$ ends of each variant sequence. For computational efficiency, we perform bidirectional prompting only on the reference sequence. These prompts are then applied consistently across all associated variant sequences.

Step 1: Input DNA Sequence. The input DNA sequence is represented as a series of states in a Markov chain model. The main strand of the DNA sequence is defined in Figure 10. This sequence corresponds to the states $x_1, x_2, x_3, \ldots, x_t$ of the Markov chain. The model processes the sequence by transitioning from one state to the next.

Step 2: DNA Double-Strand Representation. Using the initial sequence, the model generates both the main and reverse complement (RC) strand. The RC strand is derived by replacing each base in the main strand with its complement, shown in Figure 11. The corresponding Markov chain states are given by $x_1, x_2, \ldots, x_t$ for the main strand and $\hat{x}_1, \hat{x}_2, \ldots, \hat{x}_t$ for the RC strand.

Step 3: Generating Downstream of the Reverse Complement Strand. To generate the downstream sequence of the reverse complement strand, the model applies transitions based on previous transition probabilities. The downstream sequence is generated as shown in Figure 12.

Step 4: Mapping the Generated Reverse Complement Bases to the Main Strand. Finally, the model maps the generated bases of the reverse complement strand back to the main strand. This is done using mapping rules derived from the transitions in the Markov model shown in Figure 13.

D Supplemented RNA Experiments

In this section, we introduce the re-implementation details of RNAGym [4] in Section D.1, and discuss the direct prediction without ensemble in Section D.2.

D.1 Difference of Re-implementation and Official Results

As shown in Table 6, different models were inconsistently reported—Evo1.5 with direct prediction and Evo2-7B with reverse complement (RC) ensemble. Since we observed that RC ensembling has a non-trivial effect, we re-implemented all Evo1 [36], Evo1.5 [34], and Evo2 [11] baselines and reported ensemble results for fairness in the main text.

Figure 13: Mapping the generated bases of the reverse complement to the main strand.

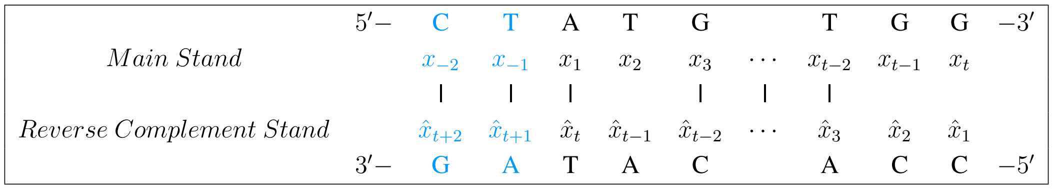

$5'-$ C T A T G T G G $-3'$
Main Stand
x_{-2} x_{-1} x_1 x_2 x_3 $\cdots$ x_{t-2} x_{t-1} x_t
Reverse Complement Stand
$\hat{x}_{t+2}$ $\hat{x}_{t+1}$ $\hat{x}_t$ $\hat{x}_{t-1}$ $\hat{x}_{t-2}$ $\cdots$ $\hat{x}_3$ $\hat{x}_2$ $\hat{x}_1$
$3'-$ G A T A C A C C $-5'$

Algorithm 1 Pseudocode of the BasePrompt Algorithm

```
Input:
    $S_{rna}$   // The source RNA sequence.
    $N$   // The target prompt length for each side.
    $GLM$   // A pre-trained Genome Language Model (generates from 5' to 3').
    Helper Functions:
    function RNAtoDNA($S_{in}$): Converts RNA sequence $S_{in}$ to DNA (U $\to$ T).
    function RevComplement($S_{in}$): Returns the reverse complement of a DNA sequence.
    function Generate($S_{in}, N, GLM$): Extends $S_{in}$ and returns only the newly generated part.
Output: The full sequence $S_{full}$, and the generated prompts $S_{5'}$ and $S_{3'}$

1: function BasePrompt($S_{rna}, N$)
2:     $S_{main} \leftarrow$ RNAtoDNA($S_{rna}$)                  ▷ Main strand, 5' to 3'

   // Phase A: 5' Prompt utilizing the complementary strand
3:     $S_{rc} \leftarrow$ RevComplement($S_{main}$)              ▷ Complement strand, 5' to 3'
4:     $S_{up,rc} \leftarrow$ Generate($S_{rc}, N, GLM$)          ▷ Upstream part on complement strand, 5' to 3'
5:     $S_{5'} \leftarrow$ RevComplement($S_{up,rc}$)             ▷ Final 5' prompt on main strand, 5' to 3'

   // Phase B: 3' Prompt (autoregressive)
6:     $S_{prefix} \leftarrow S_{5'} + S_{main}$                  ▷ Main strand, 5' to 3'
7:     $S_{3'} \leftarrow$ Generate($S_{prefix}, N, GLM$)         ▷ Final 3' prompt on main strand, 5' to 3'

   // Final Assembly
8:     $S_{full} \leftarrow S_{5'} + S_{main} + S_{3'}$
9:     return $S_{full}, S_{5'}, S_{3'}$
10: end function
```

D.2 Experiments of Direct Prediction w/o Ensemble

As shown in Table 7, BasePrompt performs well even using only direct prediction without ensembles. We use the reverse complement ensemble for both baselines and ours on the Evo series, following the Evo2 setting of RNAGym. It demonstrates the generality of our method. The prompt lengths of BasePrompt for models on the table from top to bottom are 32, 32, 3, 2, and 5.

D.3 Performance across Models at a Prompt Length of Three

As shown in Table 8, we set the prompt length of BasePrompt to three and show that all models have a great performance. Although the result does not demonstrate the best performance for each model, the steady improvement demonstrates the stability of our BasePrompt. Note that we use the reverse complement ensemble for both baselines and ours on the Evo series following RNAGym. Details about direct predictions and reverse complement ensemble can be found in Table 6.

We also compare the performance across RNA types in Table 9 at a prompt length of three. Notably, BasePrompt shows improvements across all RNA types with the Evo2 40B model. In terms of model differences, BasePrompt demonstrates significant gains in mRNA splicing and mRNA coding, highlighting the potential of RNA prompting for mRNA-related functions. For the remaining three RNA types, RNA FM outperforms BasePrompt, indicating the importance of incorporating RNA-specific information. A promising future direction could involve exploring ways to integrate RNA-

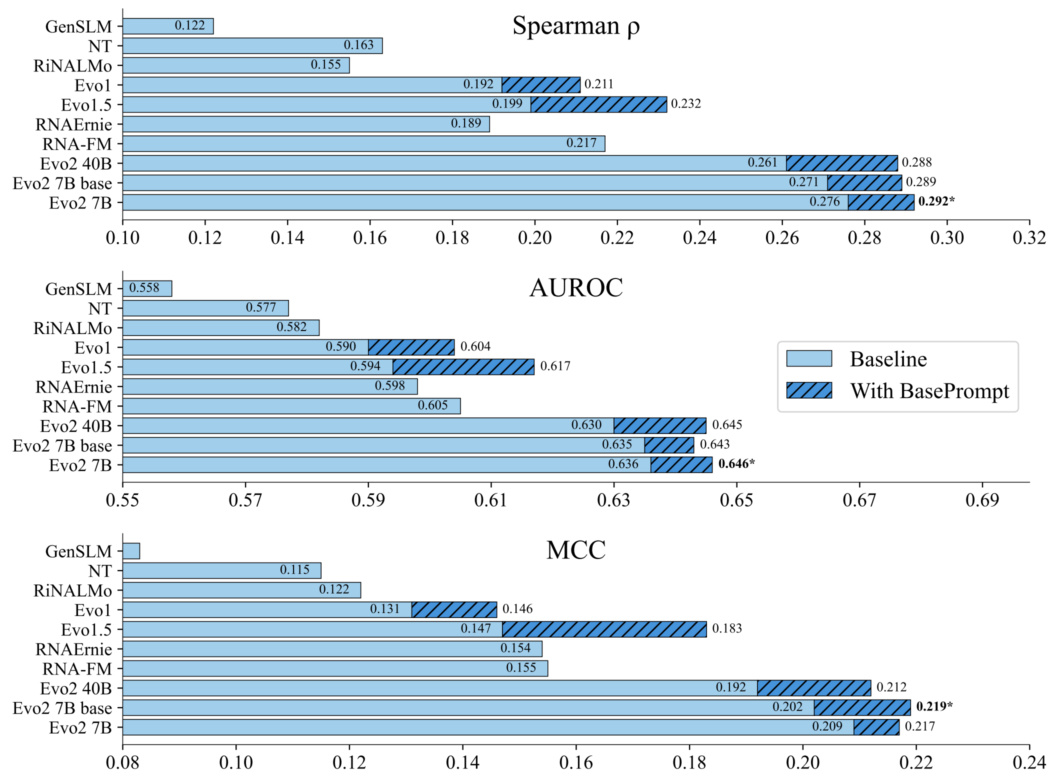

Figure 14: BasePrompt improves performance across diverse models and achieves SOTA results on the RNAGym benchmark. Results of each model's best prompt length are reported. We use the reverse complement ensemble following RNAGym on the Evo series.

related data into RNA prompting, such as leveraging RNA language models to generate upstream and downstream prompts with BasePrompt.

D.4 Performance at Best Prompt Lengths

As illustrated in Table 2, our method achieves relative improvements of 6.0–16.4% in Spearman ρ, 1.2–3.9% in AUROC, and 4.0–24.3% in MCC over the respective baseline models. We use the reverse complement ensemble for both baselines and ours on the Evo series, following the Evo2 setting of RNAGym. It demonstrates the generality of our method. The prompt lengths of BasePrompt for models on the table from top to bottom are 32, 32, 5, 3, and 5. We also show the tendency of relative improvement in Figure 14. The height of our increase in purple is much higher across three metrics.

E Supplemented DNA Experiments

In this section, we introduce several supplemented DNA experiments. We conduct experiments across a wide range of input sequence lengths for the next-base prediction task[7]. In the following experiments, we will demonstrate the general effectiveness of our BasePrompt across various (1) input lengths, (2) genome language models, and (3) sampling strategies.

BasePrompt consistently improves accuracy across different prompt lengths. As illustrated in Figure 15, BasePrompt performs well across a range of input sequence lengths and target sequence lengths. Given the substantial variability in absolute accuracy with respect to input sequence length, we present the accuracy improvement, defined as $\frac{ACC_{BasePrompt}-ACC_{baseline}}{ACC_{baseline}} \times 100\%$, to facilitate a direct comparison across different prompt lengths. The baseline values in Figure 15 correspond to

[7]Dataset version.

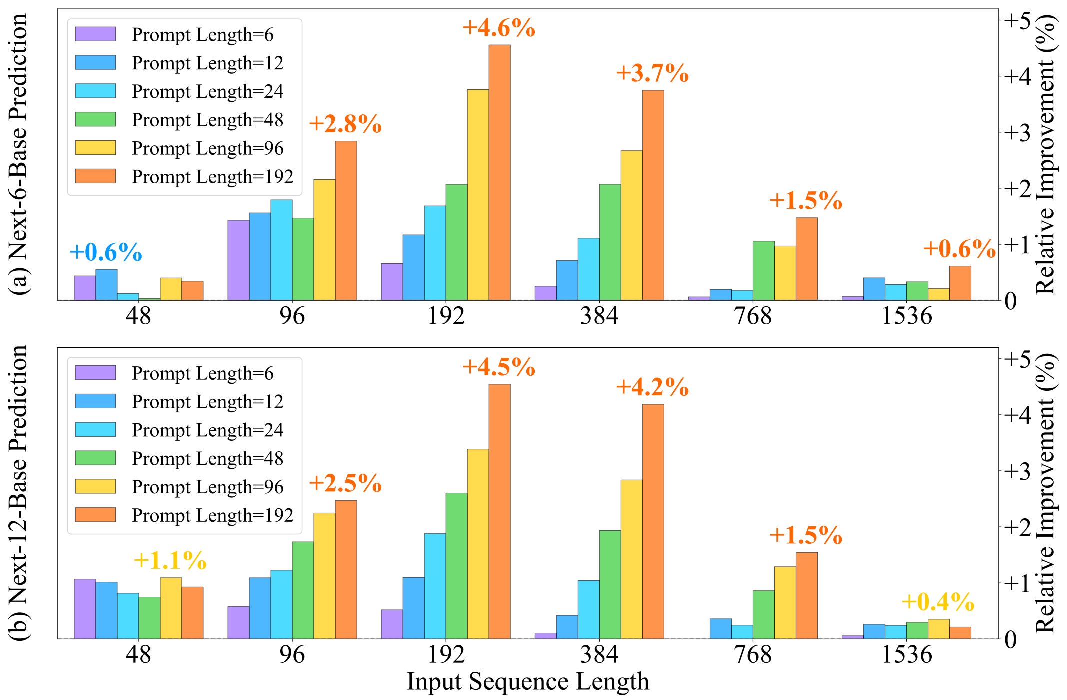

Figure 15: BasePrompt consistently enhances next-base prediction performance across varying input sequence lengths. As the input length increases, the relative accuracy gain over the baseline (original input) also grows. Panels (a) / (b) show the relative improvement results using the GENERator 3B model for predicting the next 6 / 12 bases given the input sequence, respectively.

the original input sequence, with $ACC_{baseline}$ values of 32.8%, 35.6%, 40.1%, 45.7%, 52.3%, and 56.6% for increasing prompt length, respectively. Notably, the greatest improvements are observed for mid-range input sequence lengths. This result aligns with expectations, as shorter input sequences may lack sufficient information to generate accurate prompts during inference.

BasePrompt demonstrates broad efficacy across diverse model families. We evaluate BasePrompt on both the Evo2 and GENERator families, tasked with predicting the next 6 bases from a 192-base sequence, as summarized in Table 10. For both families, sequences utilizing our prompts consistently outperform their corresponding baselines, defined as raw DNA input. Notably, BasePrompt 's effectiveness is evident across a range of model sizes, from 1.2B to 40B parameters, highlighting its robustness and lack of dependence on a specific model capacity. Furthermore, the improvement over the baseline tends to be more pronounced in larger models, underscoring that BasePrompt can leverage advancements in genome language models.

BasePrompt is robust across diverse sampling hyperparameters. We perform a comprehensive evaluation across various sampling hyperparameters, shown in Table 11. Such a sampling process influences both the bidirectional prompting and the next-base prediction task. Our method consistently performs well across a range of temperatures, top-k, and top-p values. Here, the symbol "/" denotes a neutral setting, *i.e.*, no restriction in the sampling process (top-$k = 0$ and top-$p = 1$). As top-k and top-p increase, the sampling flexibility increases, followed by a notable drop in next-base prediction accuracy. However, BasePrompt can still steadily work on such variable sampling settings, and effectively facilitate the generation task.

The Python implementation of baseline prompting modes is shown as follows:

```
def generate_prompts(mode:str, sequences: List[str], new_length: int):
    if mode == "RandomSeq":
        prompts = [
            "".join(random.choice(seq) for _ in range(new_length))
            for seq in sequences
        ]
    elif mode == "RandomBase":
        prompts = [
            "".join(random.choice('TAGC') for _ in range(new_length))
            for _ in range(len(sequences))
        ]
    elif mode == "Repeat":
        prompts = []
        for seq in sequences:
            temp_prompt = ""
            while len(temp_prompt) < new_length:
                temp_prompt = temp_prompt + seq[-new_length:]
            prompts.append(temp_prompt[-new_length:])
    elif mode in ["A", "T", "C", "G"]:
        prompts = [
            mode * new_length for _ in range(len(sequences))
        ]
    else:
        raise ValueError(f"Invalid mode: {mode}")
    return prompts
```

Table 4: We provide details on deep mutational scanning assays in RNAGym [4], complementing the information on each RNA assay that is not included in the original paper.

RNA Type	Dataset	Sequence Number	Sequence Length
Aptamer (Target binding ability)	Tome_2014_GFP_aptamer	417	82
	Tome_2014_NELFE_aptamer	2652	70
Ribozyme (Cleavage and splicing)	Andreasson_2020_ribozyme	7343	74
	Beck_2022_ribozyme	21321	69
	Janzen_2022_fam1a1_ribozyme	1953	71
	Janzen_2022_fam1b1_ribozyme	1953	71
	Janzen_2022_fam21_ribozyme	1953	71
	Janzen_2022_fam22_ribozyme	1953	71
	Janzen_2022_fam31_ribozyme	1953	71
	Kobori_2015_ribozyme_j12	255	230
	Kobori_2015_ribozyme_p4	255	190
	Kobori_2015_ribozyme_tw	1023	77
	Kobori_2016_osa_ribozyme	10296	54
	Kobori_2018_ribozyme	16383	160
	McRae_2024_5tu_ribozyme	74942	152
	McRae_2024_t1_ribozyme	47503	135
	Peri_2022_ribozyme	16383	197
	Pitt_2010_ribozyme	186	87
	Roberts_2023_HDV_ribozyme	33930	87
	Roberts_2023_cepeb3_ribozyme	21321	69
	Roberts_2023_hh_ribozyme	9045	45
	Roberts_2023_hp_ribozyme	22578	71
	Roberts_2023_tw_ribozyme	10296	48
	Soo_2021_ribozyme	64019	425
	Zhang_2020_cpeb3_ribozyme	111417	81
	Zhang_2024_OR4K15_ribozyme	61393	140
	Zhang_2024_line1_full_ribozyme	69583	146
	Zhang_2024_line1_mini_ribozyme	149710	46
	A0A2Z5U3Z0_9INFA_Doud_2016	10715	1698
mRNA Coding (Coding mRNA fitness)	BCHB_CHLTE_Tsuboyama_2023_2KRU	1652	156
	BLAT_ECOLX_Firnberg_2014	4783	861
	BLAT_ECOLX_Jacquier_2013	989	861
	BRCA1_HUMAN_Findlay_2018	886	5592
	C6KNH7_9INFA_Lee_2018	10754	1701
	CALM1_HUMAN_Weile_2017	1813	450
	CAPSD_AAV2S_Sinai_2021	42328	2208
	CBS_HUMAN_Sun_2020	7217	1656
	CCDB_ECOLI_Adkar_2012	1176	306
	DLG4_RAT_McLaughlin_2012	1576	2175
	DOCK1_MOUSE_Tsuboyama_2023_2M0Y	3099	198
	ESTA_BACSU_Nutschel_2020	2172	639
	F7YBW8_MESOW_Ding_2023	7922	282
	GFP_AEQVI_Sarkisyan_2016	51714	717
	HECD1_HUMAN_Tsuboyama_2023_3DKM	6835	216
	IF1_ECOLI_Kelsic_2016	1367	219
	MLAC_ECOLI_MacRae_2023	4007	636
	MTHR_HUMAN_Weile_2021	12464	1971
	OBSCN_HUMAN_Tsuboyama_2023_1V1C	3421	195
	OXDA_RHOTO_Vanella_2023_activity	6396	1092
	P53_HUMAN_Kotler_2018	1048	1182
	PKN1_HUMAN_Tsuboyama_2023_1URF	1305	213
	POLG_DEN26_Suphatrakul_2023	16897	2700
	POLG_PESV_Tsuboyama_2023_2MXD	6287	159
	PSAE_PICP2_Tsuboyama_2023_1PSE	1616	204
	PTEN_HUMAN_Mighell_2018	7260	1212
	Q837P4_ENTFA_Meier_2023	697	1770
	R1AB_SARS2_Flynn_2022	5725	918
	RCRO_LAMBD_Tsuboyama_2023_1ORC	2401	189
	RDRP_I33A0_Li_2023	12003	2271
	RNC_ECOLI_Weeks_2023	4277	681
	SPIKE_SARS2_Starr_2020_binding	3802	3822
	SPTN1_CHICK_Tsuboyama_2023_1TUD	3485	180
	SR43C_ARATH_Tsuboyama_2023_2N88	1663	144
	SUMO1_HUMAN_Weile_2017	1700	306
	TAT_HV1BR_Fernandes_2016	1577	258
mRNA Splicing (Splicing ability)	Julien_2016_mRNA	189	63
	Ke_2017_mRNA	5559	51
tRNA (Stability and growth)	Domingo_2018_tRNA	4175	72
	Guy_2014_tRNA	25491	105
	Li_2016_tRNA	65536	72

Table 5: Information of the Next-base Prediction dataset.

Subset	Taxomony / Species Type	Size
Eukaryote	Archaea, Viruses, Bacteria, Eukaryota	29,944
Bacteria	Bacteria	30,801
Others	Mitochondrion, Archaea, Plasmid, Virus, Plastid	23,903

Table 6: Effect of reverse-complement (RC) ensembling on RNAGym. Gray rows highlight the RNAGym-reported results and our corresponding re-implementation under the same setting. RNAGym reports Evo1.5 using direct prediction but Evo2 7B with RC ensemble, introducing inconsistency and bias in the benchmark. Our re-implementation evaluates both settings.

Model	Setting	Spearman ρ	AUROC
Evo1.5	RNAGym reported	0.177	0.583
	Our re-impl. (direct)	0.177	0.583
	Our re-impl. (+ RC ensemble)	0.199	0.594
Evo2 7B	RNAGym reported	0.276	0.636
	Our e-impl. (direct)	0.251	0.622
	Our re-impl. (+ RC ensemble)	0.276	0.636

Table 7: Our BasePrompt improves RNAGym when using direct prediction without reverse complement ensemble. Specifically, our method achieves relative improvements of 7.2–29.6% in Spearman ρ, 1.6–5.5% in AUROC, and 7.8–31.7% in MCC over the respective baseline models. Note that the baseline results of Evo2 [11] are different from RNAGym [4] since RNAGym uses both the forward and the reverse chain for function prediction. Results of each model's best prompt length are reported.

Model Name	Spearman $\rho \uparrow$	AUROC $\uparrow$	MCC $\uparrow$
RNA-FM	0.217	0.605	0.155
RNAErnie	0.189	0.598	0.154
Nucl. Transformer	0.163	0.577	0.115
RiNALMo	0.155	0.582	0.122
GenSLM	0.122	0.558	0.083
Evo1	0.175	0.587	0.135
w/ BasePrompt	0.205	0.601	0.156
Evo1.5	0.177	0.583	0.129
w/ BasePrompt	0.229	0.615	0.170
Evo2 7B base	0.257	0.626	0.194
w/ BasePrompt	0.281	0.637	0.209
Evo2 7B	0.251	0.622	0.176
w/ BasePrompt	0.269	0.633	0.210
Evo2 40B	0.264	0.630	0.195
w/ BasePrompt	**0.286**	**0.641**	**0.216**

Table 8: BasePrompt improves performance across diverse models and achieves state-of-the-art results on the RNAGym [4] benchmark. We use the reverse complement ensemble for both baselines and ours on the Evo series. Gray rows denote our method, while bold numbers highlight the best performance. The prompt length is set to three on both sides.

Model Name	Spearman $\rho \uparrow$	AUROC $\uparrow$	MCC $\uparrow$
RNA-FM	0.217	0.605	0.155
RNAErnie	0.189	0.598	0.154
NT	0.163	0.577	0.115
RiNALMo	0.155	0.582	0.122
GenSLM	0.122	0.558	0.083
Evo1	0.192	0.590	0.131
w/ BasePrompt	0.202	0.595	0.135
Evo1.5	0.199	0.594	0.147
w/ BasePrompt	0.205	0.597	0.147
Evo2 7B base	0.271	0.635	0.202
w/ BasePrompt	0.289	0.642	0.210
Evo2 7B	0.276	0.636	0.209
w/ BasePrompt	**0.292**	**0.646**	**0.217**
Evo2 40B	0.261	0.630	0.192
w/ BasePrompt	0.278	0.639	0.203

Table 9: The average Spearman's rank correlation of BasePrompt scores across various RNA types. Our method demonstrates significant improvements in mRNA splicing and mRNA coding, while RNA FM outperforms in the remaining types. Both our method and the baselines use the reverse complement ensemble in the Evo series, consistent with the Evo2 setting of RNAGym. Gray rows represent our results, with bold numbers highlighting the best performance. The prompt length of each model is three.

Model Name	mRNA-splic.	tRNA	Aptamer	Ribozyme	mRNA-cod.	Average
RNA FM	0.103	**0.464**	**0.190**	**0.201**	0.129	0.217
RNAErnie	0.230	0.416	0.037	0.142	0.117	0.189
NT	0.121	0.317	0.146	0.147	0.083	0.163
RiNALMo	0.348	0.260	0.026	0.072	0.070	0.155
GenSLM	0.173	0.093	0.126	0.135	0.084	0.122
Evo1	0.142	0.422	0.067	0.150	0.177	0.192
w/ BasePrompt	0.188	0.409	0.080	0.153	0.179	0.202
Evo 1.5	0.146	0.430	0.082	0.164	0.173	0.199
+ w/ BasePrompt	0.179	0.424	0.085	0.164	0.173	0.205
Evo2 7B Base	0.387	0.420	0.079	0.186	0.284	0.271
+ w/ BasePrompt	0.435	0.427	0.136	0.159	0.287	0.289
Evo2 7B	0.432	0.387	0.119	0.170	0.271	0.276
+ w/ BasePrompt	**0.468**	0.413	0.140	0.167	0.274	**0.292**
Evo2 40B	0.305	0.431	0.097	0.172	0.298	0.261
+ w/ BasePrompt	0.321	0.431	0.152	0.179	**0.305**	0.278

Table 10: BasePrompt is generally effective on different models. As the prompt length increases, the performance improvement becomes more pronounced. The task is predicting the next 6 bases given a sequence of length 192. The green value represents the delta compared to the baseline.

Model	Accuracy (%) by Prompt Length					
	0 (Baseline)	6	12	24	48	96
GENERator 1.2B	38.4	38.5 (↑ 0.1)	38.4 (↑ 0.0)	38.7 (↑ 0.3)	39.0 (↑ 0.6)	39.4 (↑ 1.0)
GENERator 3B	40.1	40.3 (↑ 0.2)	40.5 (↑ 0.4)	40.7 (↑ 0.6)	40.9 (↑ 0.8)	41.6 (↑ 1.5)
Evo2 1B base	46.0	46.3 (↑ 0.3)	46.7 (↑ 0.7)	47.0 (↑ 1.0)	47.1 (↑ 1.1)	47.0 (↑ 1.0)
Evo2 7B	52.8	53.1 (↑ 0.3)	53.4 (↑ 0.6)	54.0 (↑ 1.2)	54.2 (↑ 1.4)	54.5 (↑ 1.7)
Evo2 40B	65.4	65.7 (↑ 0.3)	65.8 (↑ 0.4)	66.1 (↑ 0.7)	66.4 (↑ 1.0)	66.6 (↑ 1.2)

Table 11: BasePrompt is robust under diverse generation sampling hyperparameters. The task is predicting the next 6 bases given a DNA sequence of length 384 using GENERator-3B. The top is the default setting in our experiments. The green number is the improvement compared with the baseline.

Temp	Top-k	Top-p	Accuracy (%)	
			Baseline	BasePrompt
1.0	4	1.0	45.7	47.5+1.8
1.2	/	1.00	37.4	38.9+1.5
1.0	/	1.00	39.0	40.5+1.5
0.8	/	1.00	40.6	42.3+1.7
0.6	/	1.00	42.6	44.2+1.6
1.0	100	/	42.7	44.1+1.4
1.0	50	/	43.4	44.9+1.5
1.0	10	/	45.1	46.2+1.1
1.0	1	/	46.4	48.2+1.8
1.0	/	1.00	39.0	40.5+1.5
1.0	/	0.99	39.2	40.7+1.5
1.0	/	0.90	40.4	41.5+1.1
1.0	/	0.70	41.5	43.2+1.7

Table 12: BasePrompt enhances generation quality in the next-6-base prediction task with a 192-base input. Compared to direct prediction on raw input, it yields nearly consistent gains across models even when generating a long 5′ prompt of 192 bases. Our method yields a relative accuracy improvement of 1.3–2.4% across all models. It also achieves relative reductions of 3.1–23.3% in GC Difference and 0.5–4.8% in 2-mer JSD for most models. Results are averaged across three subsets [49] to mitigate species imbalance.

Model	Accuracy ↑		GC Difference ↓		JSD (2-mer) ↓	
	Baseline	Ours	Baseline	Ours	Baseline	Ours
GENERator 1.2B	37.7	38.5	0.0466	0.0474	0.1229	0.1204
GENERator 3B	40.0	40.9	0.0360	0.0349	0.1097	0.1044
EVO2 1B base	52.4	53.0	0.0174	0.0134	0.0872	0.0861
EVO2 7B	58.0	59.3	0.0195	0.0164	0.0709	0.0697
EVO2 40B	68.1	69.1	0.0178	0.0166	0.0504	0.0502